Optics Letters

Phase stabilization of a coherent fiber network by single-photon counting

Salih Yanikgonul,[1,2,4] Ruixiang Guo,[1] Angelos Xomalis,[3] Anton N. Vetlugin,[1] Giorgio Adamo,[1] Cesare Soci,[1,*] and Nikolay I. Zheludev[1,3]

[1]Centre for Disruptive Photonic Technologies, School of Physical and Mathematical Sciences and The Photonics Institute, Nanyang Technological University, Singapore 637371, Singapore
[2]Institute of Materials Research and Engineering, Agency for Science, Technology, and Research, Singapore 138632, Singapore
[3]Optoelectronics Research Centre and Centre for Photonic Metamaterials, University of Southampton, Southampton SO17 1BJ, UK
[4]e-mail: salih001@ntu.edu.sg
*Corresponding author: csoci@ntu.edu.sg

Received 24 October 2019; revised 20 March 2020; accepted 26 March 2020; posted 26 March 2020 (Doc. ID 381388); published 6 May 2020

Coherent optical fiber networks are extremely sensitive to thermal, mechanical, and acoustic noise, which requires elaborate schemes of phase stabilization with dedicated auxiliary lasers, multiplexers, and photodetectors. This is particularly demanding in quantum networks operating at the single-photon level. Here, we propose a simple method of phase stabilization based on single-photon counting and apply it to quantum fiber networks implementing single-photon interference on a lossless beamsplitter and coherent perfect absorption on a metamaterial absorber. As a proof of principle, we show dissipative single-photon switching with visibility close to 80%. This method can be employed in quantum networks of greater complexity without classical stabilization rigs, potentially increasing efficiency of the quantum channels.

https://doi.org/10.1364/OL.381388

Leveraging on advanced telecommunication technologies, coherent optical fiber networks provide a scalable platform for quantum light processing and quantum communication. Single-photon interference [1,2], quantum computation based on a dual-rail qubit encoding [3,4], quantum key distribution [5,6], entanglement swapping and distribution [6,7], and high-dimensional quantum state transmission [8] have already been demonstrated in fiber environment proving the feasibility of fiber-based quantum optics. Recent achievements in fabrication of fully-fiberized metamaterial packages [9] allow to extend the functionality of accessible devices for quantum light manipulation. For instance, quantum coherent perfect absorption (CPA) with plasmonic metamaterial absorber, first demonstrated in a free space [10], was shown in an optical fiber network [11]. However, to deal with phase noise—an inherent problem of fiber systems, these experiments had to employ resource demanding stabilization or elaborate data post–selection techniques [1,2,11,12].

In this paper, we develop a new method of phase stabilization by single-photon counting which is far less resource demanding, and apply it to a basic coherent network represented by a fully-fiberized Mach–Zehnder interferometer (MZI) operating at the single-photon level. We further implement this technique in a coherent optical fiber network containing plasmonic metamaterial absorber operating at CPA regime, where we achieve deterministic control of single-photon absorption probability. We show all-optical switching by driving the system between absorbing and transmitting modes, otherwise not possible in the previous experiment without stabilization.

The extreme sensitivity of optical fiber networks to thermal, mechanical, and acoustic noise [13] strongly affects measurement of coherent and indistinguishable quantum light. One way to overcome this problem is employing a feedback loop for an active phase stabilization, which requires an auxiliary laser with a distinct degree of freedom (e.g., wavelength, polarization, or temporal mode) probing the same optical path traversed by quantum light [1,2,12]. Figure 1(a) shows an example of a fiberized implementation of the single-photon MZI consisting of 50:50 beamsplitters (BS) and a phase modulator backbone, and the auxiliary phase stabilization loop. Phase fluctuations affect the intensity distribution of the light detected at the output ports of the MZI. To compensate this effect, the intensity of the auxiliary laser propagating through the MZI is used to generate a feedback signal sent to the phase modulator. The dedicated multiplexers (e.g., wavelength division multiplexers, dichroic mirrors, and polarizers), filters and photodetectors are required to isolate the feedback circuit and the quantum channel. This unavoidably degrades the quality of the quantum signal.

Alternatively, single photons themselves can be used to accomplish the same task Fig. 1(b). In the single-photon regime, the photon wavefunction acquires different phases while passing through different arms of the MZI, which affects the photon distribution at the two output ports. The very same output of the single-photon detectors (SPDs) can be used to generate the feedback signal based on the expected photon rate, and the experiment can subsequently be performed within a time window shorter than the characteristic time of the phase fluctuation. The cost for this simplicity compared to stabilization

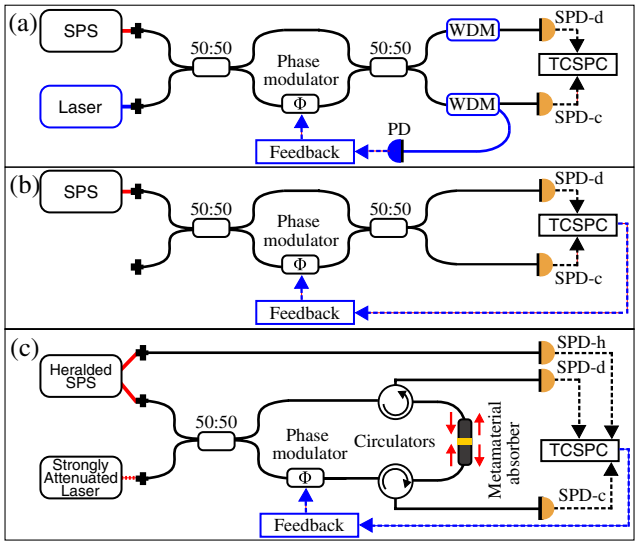

Fig. 1. Stabilization of coherent optical fiber networks operating at the single-photon level. (a) An MZI consisting of a single-photon source (SPS), 50:50 BSs, and a phase modulator as an example network. Time-correlated single-photon counting (TCSPC) module processes signals of SPDs. In conventional stabilization schemes (highlighted in blue), a laser light sent through the coherent network is separated and measured by a multiplexer (e.g., WDM) and a photodetector (PD), respectively. (b) Optical fiber networks stabilized with single photons: TCSPC output is used as an input of the feedback system. (c) Single-photon absorption control and switching experiment setup, where the second BS is substituted with a metamaterial absorber.

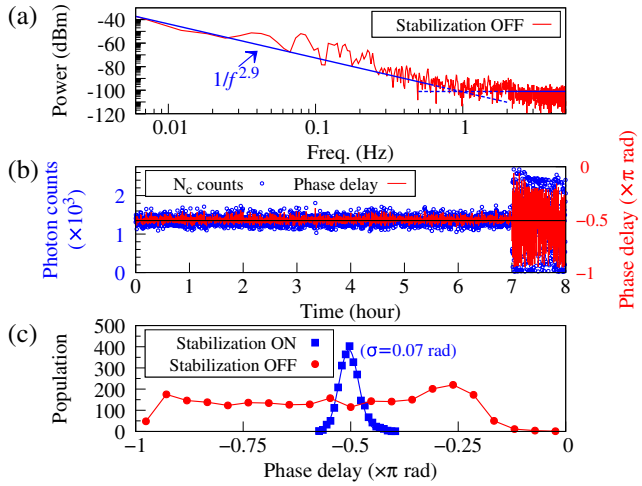

Fig. 2. Long-term phase stabilization in a fully-fiberized MZI. (a) The noise spectral density of phase fluctuations of the unstabilized system, measured by sending a CW laser of μW power through the interferometer. (b) The system is stabilized for 7 h, followed by 7 h without stabilization (only 1 h is shown). Blue circles show single-photon counts. The red line is the corresponding phase delay, and the black line is the stabilization point. (c) The corresponding phase distributions, where the blue line is the Gaussian fit curve.

schemes based on auxiliary components is: (1) lower frequency of operation as single-photon counting requires comparatively long integration time, and (2) discontinuous mode of operation, because experimental measurements are interleaved with stabilization periods.

In this Letter, first, we introduce the new phase stabilization scheme. Next, the experimental results obtained from a fully-fiberized conventional MZI stabilized with this technique is presented to show the applicability of the method to the fiberized quantum optics experiments. We conclude the paper with a demonstration of a practical application, a dissipative single-photon switch, in a quantum fiber network, which is operated at the regime of CPA and stabilized by employing this method.

To assess the phase stabilization by single-photon counting, we performed an experiment with a fully-fiberized MZI at the single-photon level [Fig. 1(b)]. In this experiment, a strongly attenuated CW laser with significantly low multiphoton states (∼200 times lower than single-photon states) is used as a single-photon source; photon wavefunction is split on a first 50:50 BS into a superposition of two spatial modes, corresponding to the upper and lower arms of the interferometer (each arm is composed of ∼15 meters of polarization-maintaining single-mode fibers). Due to the interference on the second BS, probabilities to detect a photon by SPD-c (p_c) and SPD-d (p_d) depend on the phase retardation (ϕ) between two optical paths, [11]

$$p_c(\phi) = (1 + \sin(\phi))/2$$
$$p_d(\phi) = (1 - \sin(\phi))/2. \quad \textbf{(1)}$$

To estimate these probabilities, the counts of SPD-c (N_c) and SPD-d (N_d) should be measured during the time interval Δt smaller than the characteristic time of the phase noise,

$$N_c(\phi) = N \cdot p_c(\phi)$$
$$N_d(\phi) = N \cdot p_d(\phi), \quad \textbf{(2)}$$

where N is the number of photons arriving at the second BS during Δt. In our experiments, the phase noise is caused by thermal noise affecting optical fibers and electronic noise associated with the single-photon counting unit as described in [14,15], respectively. The noise spectral density [Fig. 2(a)] decreases by $1/f^{2.9}$ until 1 Hz beyond which a broadband noise having < -100dBm power dominates. Because the noise is present on a scale of $\Delta f_N \approx 1$ Hz without significant contributions above this frequency, we set $\Delta t = 24$ ms ($\Delta t \ll 1/\Delta f_N$).

Because ϕ is the only parameter that determines the detected photon numbers N_c and N_d, we may monitor the phase stability of the network by measuring the variation of SPD counts. After scanning the phase to set N_c at approximately the $N/2$ level, we start the stabilization procedure to keep N_c at the same level. This is achieved by an ad hoc digital feedback controller. If no significant phase fluctuations are present during Δt, then N_c does not change (more precisely, the number of detected photons would be within the Poisson distribution centered at $N/2$, considering the random nature of the laser source), and no action is required. Conversely, if noise causes significant phase fluctuations during Δt, and the difference $\Delta N = N_c - N/2$ becomes noticeable, a feedback voltage proportional to $-\Delta N$ is generated to offset the phase modulator driving voltage and compensating the fluctuations. The response time of the feedback loop is on the order of a few milliseconds.

The continuous stabilization of this method has been tested up to 7 h [Fig. 2(b)]. Each blue circle in Fig. 2(b) shows the number of single photons detected by the SPD-c during Δt with a sampling period of 10 s, while the red line represents the phase

delay retrieved from these counts. The corresponding distribution for the unstabilized and the stabilized periods are shown in Fig. 2(c) together with the Gaussian fit-curve with the rms width of $\sigma = 0.07$ rad for the latter. This implies that the length difference between arms of the interferometer is kept within 10 nm range for 810 nm input photons, which corresponds to a nine orders-of-magnitude spatial resolution for 15 m of fibers. This value is comparable to those demonstrated in conventional stabilization schemes [1,2,12], which demonstrates the possibility of controlling single photons by single-photon counting in coherent optical fiber networks. (Fig. 2) clearly shows that the stabilization of the network is necessary for long-term operation of the interferometer (beyond 1 s). We note that the stabilization of longer interferometers with enlarged noise bandwidth may require a decrease of the integration time (Δt) and increase of the single-photon source brightness.

Next, to prove the applicability of this new technique to fiberized quantum optics experiments, we measured single-photon interference fringes according to Eqs. (1) and (2), Fig. 3(a), in the stabilized MZI [Fig. 1(b)]. The N_c is first set at the $N/2$ level, and the system is stabilized at this point, which requires to set some phase retardation (ϕ_{st}) by the phase modulator. Then, the feedback is switched off, and the phase retardation is shifted to one from a discrete set,

$$\phi_n = \phi_{st} + n \cdot \Delta\phi, \tag{3}$$

where $\Delta\phi \approx 0.1\pi$ and $n = 0, \pm1, \pm2, \ldots$ during time interval Δt. The corresponding photon number detected by SPD-c and SPD-d, $N_c(\phi_n)$ and $N_d(\phi_n)$, is recorded. After that, the phase retardation is stabilized back to ϕ_{st}. In this way, a 2π phase spectrum is sampled. In addition to this static stabilization in which the set point is fixed (i.e., $N/2$), we note that the proposed technique can be extended to dynamical stabilization, performed at any point of the SPD-c curve without any need to go back to ϕ_{st} after each measurement, or to a Pound–Drever–Hall type of phase control [16] by periodically modulating phase retardation with an extra phase modulator.

The experimental data [Fig. 3(a)] clearly demonstrate out-of-phase oscillation of N_c and N_d as it is expected according to theoretical predictions of Eqs. (1) and (2). This verifies an ability to manipulate quantum light in a coherent quantum network without a necessity to complicate the setup.

Last, we show that a phase stabilized coherent fiber network operating at CPA regime can be used to control the single-photon absorption probability for coherent optical switching. Unlike conventional optical switches based on nonlinear processes that require high light intensity, interferometric switches operate down to the single-photon level and are therefore suitable for quantum optics applications. Compared to a standard Mach–Zehnder intensity modulator which only redistributes the light between two outputs; CPA switching has the additional advantage of complete light dissipation. Thus, CPA interferometers can be used in complex coherent networks because they prevent the propagation of residual, undesired photons. Furthermore, CPA interferometers can also be used as quantum state filters [17].

In our experiment, the CPA takes place in a setup shown in Fig. 1(c), when the output 50:50 BS is replaced by a coherent perfect absorber. This lossy component can be described by a four-port device with

$$t = \pm r = 1/2, \tag{4}$$

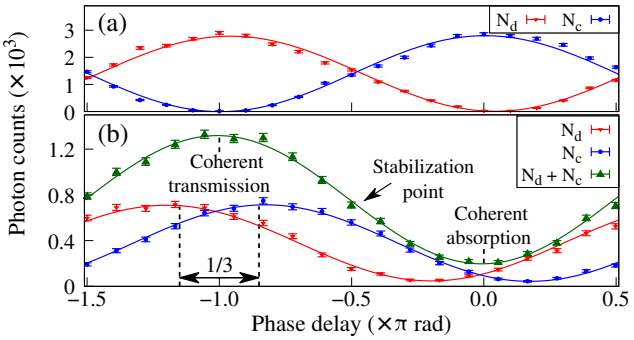

Fig. 3. Single-photon manipulation in coherent optical fiber networks stabilized by single photons. (a) Single-photon interference in a fully-fiberized MZI [Fig. 1(b)]. (b) Single-photon absorption control with a CPA [Fig. 1(c)]. Each point corresponds to a single measurement; the dispersion is defined by the Poisson distribution.

where t and r are amplitude transmission and reflection coefficients, respectively. In contrast to Eq. (1), the photon detection probability at output ports of the absorber here is defined as [11]

$$p_c(\phi) = p_d(\phi) = (1 - \cos\phi)/4, \tag{5}$$

with a total absorption probability, $1 - (p_c + p_d)$, varying in the range from 0 to 1. Recently, the CPA at the single-photon level was demonstrated in a fully-fiberized optical fiber network [11], using advanced data postselection to overcome the phase noise. This data postselection technique, however, did not allow to determine the absorption probability of single photons on demand, which our new technique is capable of.

Similar to the previous experiment, Fig. 1(c), we use two independent single-photon sources: (1) a strongly attenuated CW laser at a wavelength of 810 nm, and (2) a heralded single-photon source based on degenerate spontaneous parametric down-conversion (SPDC) in a nonlinear crystal (BBO) pumped by a CW laser at a wavelength of 405 nm. We use an attenuated laser source to measure the interference fringes, and we use the heralded source to demonstrate single-photon switching beyond the dark count noise. In the latter case, the detection of an idler photon of SPDC source by the single-photon detector SPD-h heralds the presence of the signal photon, which is sent to a optical fiber network through a 50:50 BS. The second input port of the BS is used to launch photons from the attenuated laser. The coherent optical fiber network is comprised of an MZI where a delay line (to equal the interferometer arms within 100 μm of the coherence length of the heralded photons) and a fiber stretcher (used as a phase modulator) are inserted in the bottom arm, and a variable attenuator is placed in the upper arm to equal the losses in the optical paths (not shown for simplicity). To separate photons propagating in different directions, circulators are used in both arms of the interferometer. After splitting on the first input 50:50 BS, the photon is recombined in the middle of the network, where a fully-fiberized coherent perfect absorber is placed. To fabricate the coherent absorber with the desired parameters [Eq. (4)], we exploit split-ring resonator structure manufactured on a 50 nm thick gold film deposited on the end-facet of the optical fiber (for details see [11,18]).

In Fig. 1(c), the length of each arm of the interferometer is ~20 m. The phase noise is similar to the one shown in Fig. 2(a), thus we keep $\Delta t = 24$ ms. Because the outputs of the absorber

are expected to behave in phase [Eq. (5)], we use the total counts of SPD-c (N_c) and SPD-d (N_d) measured during Δt

$$N_c + N_d = N \cdot (1 - \cos\phi)/2, \tag{6}$$

as a reference signal for the stabilization. Here N is the number of photons impinging on the absorber during Δt.

The interference fringes are measured following the stabilization of the system. Our experimental results [Fig. 3(b)] show that N_c and N_d oscillate almost in phase (with a shift of $\pi/3$), which is in a good agreement with the expected results according to Eqs. (5) and (6). The $\pi/3$ phase shift is due to the imperfections in the device fabrication and in-phase behavior can be obtained by fabricating the metasurface symmetrically or by using a matching gel inside the metadevice package [11].

During a 2π-phase scan, the system passes the regimes of coherent absorption (minimum of the $N_c + N_d$ counts, $N_{\min}$) and coherent transmission (maximum of the $N_c + N_d$, $N_{\max}$) with visibility of $(N_{\max} - N_{\min})/(N_{\max} + N_{\min}) = 73\%$. This visibility is lower than the visibility of individual curves (89% for N_c and 86% for N_d) due to the aforementioned nonideality of the sample, and the unity system visibility is achievable if the device nonideality is mitigated.

This result is close to the one demonstrated previously [11]. Nonetheless, thanks to the new stabilization scheme, now we are able to control the absorption probability on-demand, which is crucial for practical applications of CPA phenomenon in quantum light processing. In this regard, we implement a dissipative single-photon switch as a proof of principle application. Here, we use the heralded single-photon source for data acquisition to overcome the dark count noise. After each stabilization cycle, the system is driven to either the coherent absorption or transmission regime [Fig. 4(a)], and the coincidence counts of SPD-c and SPD-h and SPD-d and SPD-h are recorded during Δt [Fig. 4(b)]. The flux of photons passes through the absorber at coherent transmission regimes, while it is almost totally absorbed during coherent absorption regimes. The photon distributions [Fig. 4(c)] correspond to Poisson statistics of randomly generated heralded photons, where the data are acquired from 300 transmission and absorption cycles. On average, eight photons with a standard deviation (sd) 2.8 are detected during the transmission cycle and one photon with a sd 1.0 is detected during the absorption cycle, with a switching visibility of 78%.

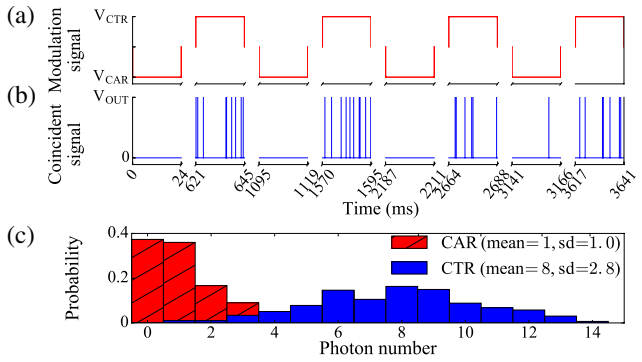

Fig. 4. Dissipative single-photon switching. (a) The modulation signal drives the system between coherent absorption (CAR) and transmission regimes (CTR). (b) The coincident photon detection signal of SPD-c and SPD-h and SPD-d and SPD-h. [(a) and (b) share the x axis, of which broken parts correspond to phase stabilization periods]. (c) The corresponding coincidence count distributions.

In summary, we showed a simple yet powerful technique of phase stabilization of coherent optical fiber networks based on single-photon counting. The method is able to overcome the phase noise inherent in optical fiber systems with no need for auxiliary laser and additional optical components required in conventional approaches. Achieved phase stability of 0.07 rad allowed us to control single-photon absorption on-demand in a fully fiberized MZI. Moreover, the method applied to a quantum network operating in the regime of the CPA made possible to realize dissipative switching at the single-photon level with visibility close to 80%. Significant hardware simplification brought about by the proposed scheme is promising. The development of relevant quantum technologies such as SPDs with a decreased dead time and high efficiency, bright sources of quantum light and high-performance integrated optics at telecom wavelengths would allow the real-world applications of this technique in coherent quantum communication and computation systems.

Funding. Singapore A*STAR QTE program (SERC A1685b0005); Ministry of Education - Singapore (MOE2016-T3-1-006 (S)); UK's Engineering and Physical Sciences Research Council (EP/M009122/1).

Acknowledgment. The authors thank Victor Leong and Rainer Dumke for technical discussions. The data from this paper are available from the University of Southampton ePrints research repository: https://doi.org/10.5258/SOTON/D1305.

Disclosures. The authors declare no conflicts of interest.

REFERENCES

1. G. B. Xavier and J. P. von der Weid, Opt. Lett. **36**, 1764 (2011).
2. S.-B. Cho and T.-G. Noh, Opt. Express **17**, 19027 (2009).
3. J. M. Lukens and P. Lougovski, Optica **4**, 8 (2017).
4. H.-H. Lu, J. M. Lukens, N. A. Peters, B. P. Williams, A. M. Weiner, and P. Lougovski, Optica **5**, 1455 (2018).
5. H. Liu, J. Wang, H. Ma, and S. Sun, Optica **5**, 902 (2018).
6. G. B. Xavier and G. Lima, Commun. Phys. **3**, 9 (2020).
7. T. Ikuta and H. Takesue, Sci. Rep. **8**, 817 (2018).
8. B. D. Lio, L. K. Oxenlowe, D. Bacco, D. Cozzolino, N. Biagi, T. N. Arge, E. Larsen, K. Rottwitt, Y. Ding, and A. Zavatta, IEEE J. Sel. Top. Quantum Electron. **26**, 1 (2020).
9. A. Xomalis, I. Demirtzioglou, E. Plum, Y. Jung, V. Nalla, C. Lacava, K. F. MacDonald, P. Petropoulos, D. J. Richardson, and N. I. Zheludev, Nat. Commun. **9**, 182 (2018).
10. T. Roger, S. Restuccia, A. Lyons, D. Giovannini, J. Romero, J. Jeffers, M. Padgett, and D. Faccio, Phys. Rev. Lett. **117**, 023601 (2016).
11. A. N. Vetlugin, R. Guo, A. Xomalis, S. Yanikgonul, G. Adamo, C. Soci, and N. I. Zheludev, Appl. Phys. Lett. **115**, 191101 (2019).
12. S.-B. Cho and H. Kim, Opt. Express **24**, 10980 (2016).
13. T. Musha, J. I. Kamimura, and M. Nakazawa, Appl. Opt. **21**, 694 (1982).
14. J. Dong, J. Huang, T. Li, and L. Liu, Appl. Phys. Lett. **108**, 021108 (2016).
15. N. Dutton, I. Gyongy, L. Parmesan, and R. Henderson, Sensors **16**, 1122 (2016).
16. E. D. Black, Am. J. Phys. **69**, 79 (2001).
17. A. N. Vetlugin, S. Yanikgonul, R. Guo, A. Xomalis, G. Adamo, C. Soci, and N. I. Zheludev, in *7th International Topical Meeting on Nanophotonics and Metamaterials: Nanometa*, Seefeld, Austria (2019).
18. A. Xomalis, I. Demirtzioglou, Y. Jung, E. Plum, C. Lacava, P. Petropoulos, D. J. Richardson, and N. I. Zheludev, Appl. Phys. Lett. **113**, 051103 (2018).